

High Flame Retardancy and High-strength of Polymer Composites with Synergistically Reinforced MOSw and EG

Chowon Kim*, Jinwoo Lee*, Hyejeong Yoon*, Jonghwan Suhr*,**†

ABSTRACT: Polymers are inherently vulnerable to flame, which limits their application to various high-tech industries. In addition, environmental regulations restrict the use of halogen-based flame retardants which has best flame-retardant effect. There are inorganic flame retardants and phosphorous flame retardants as representative non-halogen-based flame retardants. However, high content of flame retardants is required to impart high flame retardancy of the polymers, and this leads to a decrease in mechanical properties. In this research, a new approach for inorganic flame retardant-based polymer composites with high mechanical properties and flame retardancy was suggested. Inorganic flame retardants called as magnesium oxysulfate whisker (MOSw) were used in this research. MOSw can extinguish fire by releasing water and non-combustible gases when exposed to flame. In addition, they have reinforcing effect when added into the polymer with its high aspect ratio. Expandable graphite (EG) was used as a flame-retardant supplement by helping to form a more dense char layer. Through this research, it is expected that it can be applied to various industries requiring flame retardancy such as automobile, and architecture by replacing halogen-based flame polymer composites.

Key Words: Flame retardant composites, Magnesium oxysulfate whisker, Expandable graphite

1. INTRODUCTION

As flame retardants become an essential material to minimize casualties and property damage in the event of a fire, the demand for polymeric flame retardants is steadily growing. In particular, the demand for polymers which has light-weight is rapidly growing in automobile industry, as the electric vehicle market grows sharply due to the fire hazards of its lithium-ion batteries.

Halogen flame retardants, which have been widely used in many fields due to significant flame-retardant effect. However, many studies show that harmful environmental hormones and substances are released during combustion, continuing to create regulations and guidelines for the use of halogen flame retardants [1]. Therefore, a non-halogen-based polymeric flame retardants should be investigated and developed to meet these new regulations and guidelines.

Representative non-halogen flame retardants, such as phos-

phorous and metal hydroxide (inorganic) flame retardants, deteriorate mechanical properties when used as fillers, and flame retardancy is inefficient than the halogen flame retardants. In the case of phosphorus flame retardants, they have the advantage of excellent flame retardancy effects in the polymers by forming char or capturing the active radicals. However, the mechanical properties, durability and weather resistance are reduced when they added to the polymers [2].

In addition, metal hydroxide flame retardants are often used as flame retardants for electrical and electronic products due to their low cost, non-toxicity, corrosivity, and insulation, but they do not have much flame-retardant effect, requiring high filler concentration (60 wt% or more). The addition of these high content fillers results in poor dispersion and mechanical properties of the composites [3-5]. Consequently, conventional non-halogen flame retardants have fatal problem related to mechanical properties.

In this study, magnesium oxysulfate whisker (MOSw) which

Received 20 June 2022, received in revised form 14 August 2022, accepted 16 September 2022

*Department of Polymer Science and Engineering, Sungkyunkwan University

**Department of Mechanical Engineering, Sungkyunkwan University

†Corresponding author (E-mail: suhr@skku.edu)

has a high aspect ratio and high mechanical properties was used as the flame retardant of acrylonitrile-butadiene-styrene (ABS). In addition, small amount of expandable graphite (EG) which can form compact char layer than MOSw was used as supplements. As a result, a new flame-retardant composite which has high flame retardancy (V-0) and mechanical properties with a small amount of flame retardants was developed. MOSw was synthesized by hydrothermal synthesis, and its effective elastic modulus was determined by semi-empirical approach with tensile testes and a numerical model. In addition, flame retardancy and mechanical properties of the MOSw/EG/ABS composites were analyzed.

2. EXPERIMENTAL

2.1 Materials

An ABS (HF380, LG Chemical, Korea) was used as polymer matrix, and an EG (Samjung CNG, Korea) and a MOSw were used as flame retardant fillers (FRs). MgSO_4 and NaOH for synthesizing MOSw were purchased from Sigma Aldrich, USA.

2.2 Synthesis of MOSw

0.1 M Magnesium Sulfate (MgSO_4) solution and 0.1 M Sodium Hydroxide (NaOH) solution were mixed in the hydrothermal reactor. The hydrothermal reaction was carried out between about 140 and 220°C. The products obtained were washed and filtered using water. After then, it was dried at 100°C for 24 h in a vacuum oven.

2.3 Fabrication of Composites

All ABS and FRs were dried in the vacuum oven at 50°C for 3 h before use. ABS and FRs were blended together in a Haake PolyDrive mixer at 190°C for 10 min. The Table 1 shows the compositions of the composites. To prepare the tensile specimen, injection molding was used at 190°C, and the flame retardant specimen was manufactured by hot compressive

molding at 190°C for 15 min at pressure of 10 MPa.

2.4 Characterization

Thermogravimetric behaviors and functional groups of the MOSw were investigated by TGA (TG/DTA7300, SEICO INST), and FT-IR (TENSOR27, Bruker), respectively. The samples were dried in a vacuum oven before taking the tests. TGA was measured from room temperature to 1,200°C at ramp rate of 10°C/min under nitrogen atmosphere, FT-IR spectra was observed using KBr pellet method.

Flame retardancy of the composites was analyzed by the vertical burning test following ASTM D3801 and cone calorimeter according to ISO 5660. The dimension of specimen for the vertical burning test was $130 \times 13 \times 3 \text{ mm}^3$, and flame size was fixed at 20 mm during the vertical burning test. The specimen dimension for cone calorimeter test was $100 \times 100 \times 3 \text{ mm}^3$, and the specimens are exposed to external heat under heat flux of 50 kW/m^2 .

The microstructures of char residues after cone calorimeter test were taken by Scanning Electron Microscopy (SEM, IM-60, ISP, Korea), and mechanical properties of the composites were measured by Universal Testing Machine (UTM, Instron E3000). The test specimen was made following ASTM D638.

3. RESULTS AND DISCUSSION

3.1 Characterization of MOSw

3.1.1 FT-IR

FT-IR analysis was conducted to verify the presence of specific functional groups in the MOSw (Fig. 1). 1 mole of MOSw ($5\text{Mg}(\text{OH})_2 \cdot \text{MgSO}_4 \cdot 3\text{H}_2\text{O}$) is composed of 5 mol of $\text{Mg}(\text{OH})_2$, 1 mol of MgSO_4 , and 3 mol of crystalline water. OH group ($1,635 \text{ cm}^{-1}$) of crystalline water within the MOSw, OH group ($3,600\text{--}3,000 \text{ cm}^{-1}$) by $\text{Mg}(\text{OH})_2$ on the surface, and the specific vibration of sulfate ions ($1,118 \text{ cm}^{-1}$) by MgSO_4 were observed.

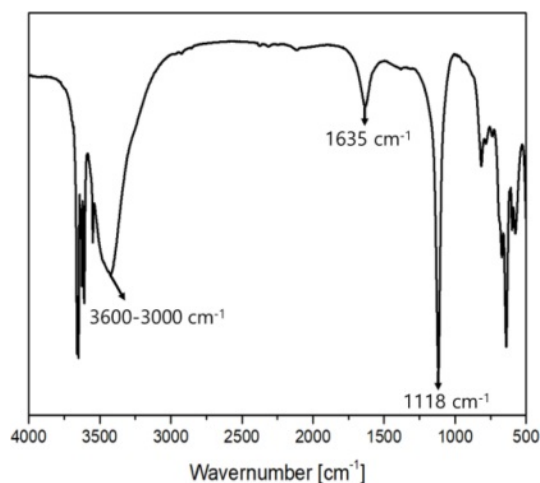


Fig. 1. FT-IR spectra of MOSw

Table 1. Compositions of the composites

Sample	Mass fraction (wt%)		
	ABS	MOSw	EG
ABS	100	-	-
MABS-1	90	10	-
MABS-2	80	20	-
MABS-3	70	30	-
MABS-4	60	40	-
EABS-1	90	-	10
EABS-2	80	-	20
MEABS-1	60	39	1
MEABS-2	60	37	3
MEABS-3	60	35	5

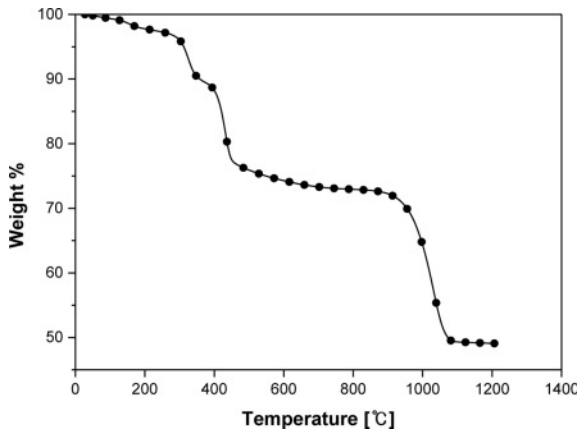


Fig. 2. Thermal behaviors of MOSw

3.1.2 TGA

TGA graph in Fig. 2 shows typical three-step mass reduction behavior of the MOSw. The first step mass reduction (200–320°C) represents a reduction due to dehydration of crystalline water in MOSw, the second mass reduction (350–420°C) is a reduction due to dehydration of OH groups on the MOSw surface, and the last mass reduction (950–1,050°C) means a reduction due to evaporation of SO_3 .

3.1.3 Morphological Observation & Determination Effective Modulus of MOSw

Due to the nano-size diameter and the micro-size length of the MOSw, there is a limitation to derive mechanical properties of MOSw itself. By adding MOSw to the polymer resin and measuring mechanical properties of the composites through tensile tests, it is possible to determine the mechanical properties of the MOSw, which is called as effective modulus.

Modified Halpin-Tsai equation (Equation (1)) was used to derive the effective modulus of MOSw, the equation is as follows:

$$\frac{E_1}{E_m} = \frac{1 + \xi \eta V_f}{1 - \eta V_f}, \text{ where } \eta = \frac{\frac{E_{f1}}{(E_m - 1)}}{\frac{E_{f1}}{(E_m + \xi)}}, \xi = \frac{2L}{d} \quad (1)$$

Where, E_m , E_{f1} , and E_1 are Young's modulus of a polymer matrix, a filler, and a composite of them, respectively. L and d mean length and diameter of the filler, and V_f is a volume fraction of the filler. The effective modulus of the filler, E_{f1} can be determined by measuring E_m and E_1 through tensile tests. Tensile test results of ABS and MABS-1 ($V_f = 0.048$) were used to

Table 2. Mechanical properties of MOSw/ABS composites

E_m [GPa]	2.26 ± 0.09
E_1 [GPa]	3.49 ± 0.05
Volume fraction of MOSw (V_f)	0.048

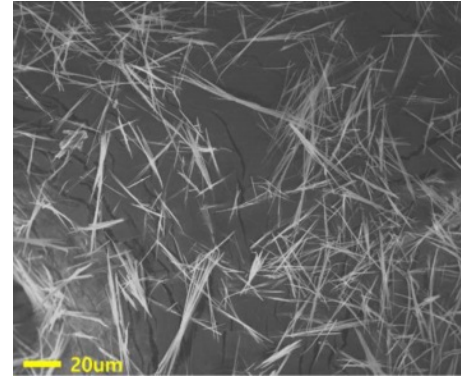


Fig. 3. SEM image of MOSw

Table 3. Morphology of MOSw

	MOSw
Length [μm]	25.5
Diameter [μm]	0.46

determine E_m and E_1 . The measured average Young's modulus values are shown in Table 2.

The L and d values of the MOSw were confirmed by checking morphology using a SEM image as shown in Fig. 3. The average L and d values are shown in Table 3.

Finally, the effective modulus of the MOSw, E_{f1} was derived as 30.4 GPa by experimentally determined values of E_m , E_1 , L , d , and V_f values.

3.2 Mechanical Properties of MOSw/ABS Composites

In addition, the effect of enhancing the mechanical properties of the MOSw was verified by tensile tests of the MOSw/ABS composites with various MOSw concentrations (MABS-1, 2, 3, 4, 5). As the concentration of MOSw increases, both Young's modulus and tensile strength were proportionally improved. However, when 30 wt% or more MOSw was added,

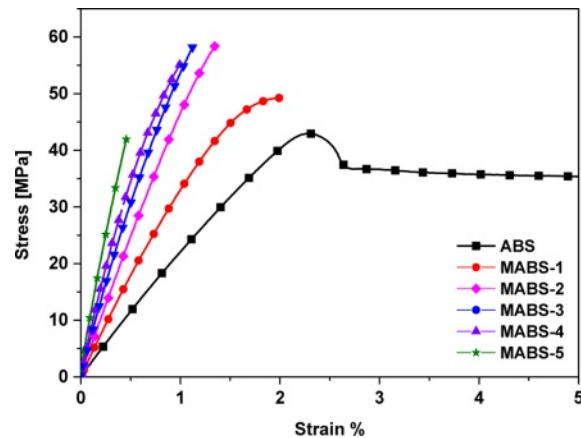


Fig. 4. Strain-Stress curve of MOSw/ABS composites

the tensile strength tended to decrease, and from the 50 wt% of MOSw was added, the tensile strength and elongation dramatically decreased. This seems to be because dispersibility of the MOSw decreases by excessive MOSws were added from 30 wt%. Low dispersibility due to the entanglement between fillers has an adverse effect on the mechanical properties of composite materials [6]. Therefore, it is considered that the optimal content of the MOSw in terms of mechanical strength should be less than 40 wt% in the MOSw/ABS composite.

3.3 Flammability

3.3.1 Vertical Burning Tests

Table 4 shows the UL-94 ratings of the ABS, MOSw/ABS composites (MABS-1, 2, 3, 4), EG/ABS composites (EABS-1, 2), and MOSw/EG/ABS composites (MEABS-1, 2, 3). When only MOSw was used, even in 40 wt% of loading fractions, UL-94 rating couldn't be achieved.

When only MOSw is used as flame retardant filler, it can be seen that large and many cracks are formed on the surface of the specimen after the vertical burning test (Fig. 5(a, b)). In addition, it was confirmed that a number of vacant spaces exist between loosely intertwined MOSws. As a result of this analysis, it is estimated that the fillers, which have a fiber shape with a high aspect ratio, such as the MOSw, have disadvantages to form a dense non-combustible layer.

In this study, EG was used as flame retardant supplements to compensate insufficient ability to form chars of the MOSw. First, char forming ability of the EG itself was evaluated. It was confirmed that the V-0 grade can be achieved at 20 wt% of the EG, and a thick layer of char by graphite expanded on the surface was formed (Fig. 5(c, d)). This result implies that the fluffy char layer composed of the EG was able to effectively prevent the penetration of the heat source into the composites.

Finally, the flame retardancy was analyzed when the MOSw and EG are charged together in the composite. The highest

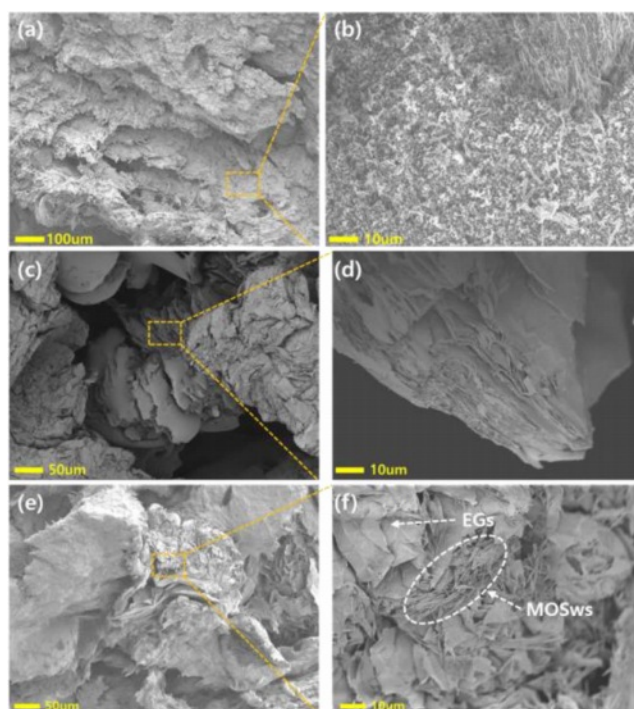


Fig. 5. SEM images of char residue after the vertical burning test ((a, b) MABS-4, (c, d) EABS-2, (e, f) MEABS-3)

flame retardancy grade, V-0 could be achieved even 5 wt% of EG was added. This indicates there is a synergistic effect of flame retardancy between MOSw and EG in the ABS composites. The char images in Fig. 5(e, f) can support this synergistic effect. It was confirmed that the MOSws were successfully entangled with EG layers. Therefore, it is believed that an effective flame retardancy could be obtained by forming a denser char structure when the EG is applied with the MOSw together than when the MOSw is used alone.

3.3.2 Cone Calorimeter Test

Cone calorimeter analysis can be performed to analyze flame retardancy quantitatively by measuring the amount of heat and smoke released during combustion. Through this analysis, a quantitative analysis of peak heat release rate (PHRR), total heat release (THR), total smoke release rate (TSR) can be measured.

Fig. 6(a, b) are the graphs of heat and total smoke release rates on ABS and FRs/ABS composites (MABS-4, EABS-2, MEABS-3). In the case of pure ABS, high heat dissipation rates were explosively recorded within a short period of time and a large amount of heat and smoke were emitted during the test. This is because ABS, which is vulnerable to heat, undergoes a combustion reaction very quickly and is pyrolyzed [7].

When only MOSw was used as flame retardant filler, the overall heat dissipation rate pattern tended to decrease. In particular, the amount of gas generated (TSR) was rapidly reduced due to the cooling effect and the combustible gas dilution

Table 4. Vertical burning test results

Sample	Mass fraction (wt%)			UL-94
	ABS	MOSw	EG	
ABS	100	-	-	NR
MABS-1	90	10	-	NR
MABS-2	80	20	-	NR
MABS-3	70	30	-	NR
MABS-4	60	40	-	NR
EABS-1	90	-	10	NR
EABS-2	80	-	20	V-0
MEABS-1	60	39	1	V-1
MEABS-2	60	37	3	V-1
MEABS-3	60	35	5	V-0

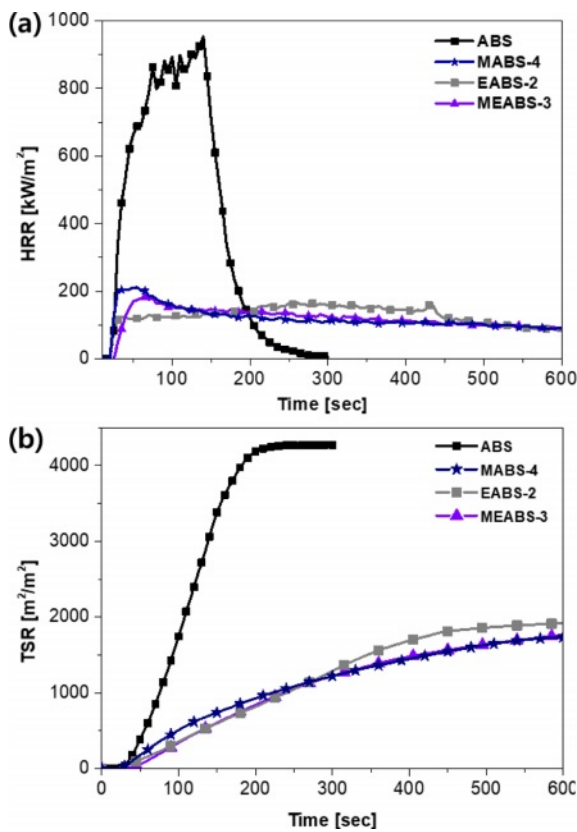


Fig. 6. Heat (a) and total smoke (b) release rate curves of ABS & FRs/ABS composites

effect generated by the pyrolysis of MOSw [8-11].

In the case of EABS-2, the maximum heat dissipation was the lowest value of 166 kW/m². This means that the thick char layer on the surface of the material formed simultaneously with the combustion. However, the amount of smoke generating was higher than that of the composites including MOSw, which means that the effect of diluting a large number of harmful gases generated from organic materials is relatively low when only EG is used.

For the MEABS-3, the maximum heat dissipation was slightly higher than that of the EABS-2, but the total heat dissipation and the average heat dissipation were the lowest among all materials. This suggests that the total amount of heat generation can be significantly reduced when MOSw is used with EG, and the combustion speed may also be slow. Therefore, when the MOSw and EG are used in the composite

Table 5. Cone calorimeter data

Sample	PHRR [kW/m ²]	THR [MJ/m ²]	Mean. HRR [kW/m ²]	TSR [m ² /m ²]
ABS	954	115	418	4270
MABS-4	211	70	122	1733
EABS-2	166	76	125	1916
MEABS-3	183	70	116	1765

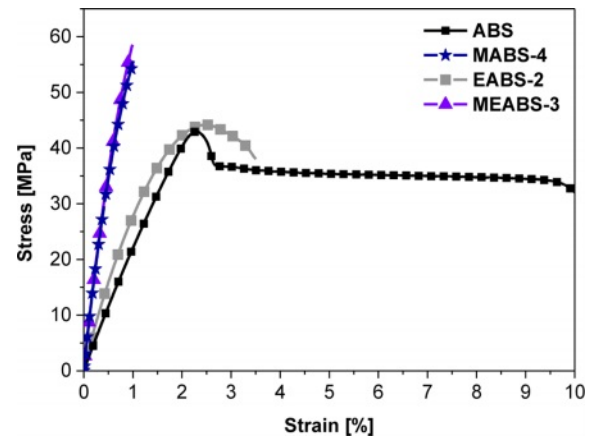


Fig. 7. Strain-Stress curves of composites

Table 6. Tensile test results of composites

	Tensile strength [MPa]	Young's modulus [GPa]	Elongation [%]
ABS	42.4 ± 0.7	2.1 ± 0.1	14.0 ± 0.6
MOSw/ABS	54.8 ± 1.2	7.7 ± 0.1	1.0 ± 0.0
EG/ABS	43.6 ± 1.9	3.4 ± 0.0	3.4 ± 0.2
MOSw/EG/ABS	55.9 ± 2.3	7.9 ± 0.1	0.9 ± 0.1

together, it can be seen that there is a synergistic effect in flame retardancy by applying a direct heat source blocking effect of the MOSw with EG and a cooling and diluting effects of the MOSw.

3.4 Mechanical Properties

A tensile test was performed to compare and analyze the mechanical properties of each composite material (Fig. 7). When the EG was added, the tensile strength and Young's modulus slightly increased compared to pure ABS, and the elongation decreased to 3.4%.

When the MOSw was added, the tensile strength (29%) and elastic modulus (267%) were significantly improved due to the high mechanical properties of the MOSw. It means the stress can be transferred effectively to the MOSw by the fiber shape with high aspect ratio.

Even when the MOSw is added to ABS with a small amount of EG, mechanical properties are comparable to the composite that only MOSw is used. It is believed that the MOSw and EG show uniform dispersion at the corresponding content.

4. CONCLUSIONS

This study includes the research of high flame retardancy as well as high-strength of polymer composites by employing the MOSw and EG together. The effect of reinforcing mechanical strength by the MOSw was determined by deriving an effec-

tive modulus using a semi-empirical approach with modified Halpin-Tsai equation and tensile tests. However, UL-94 grade was not rated when only MOSw was applied as a flame-retardant filler. This seems to be dense char layer is difficult to be formed due to high aspect ratio of the MOSw and the cooling and gas effects of MOSw itself cannot prevent effectively the very fast combustion of the polymers.

Therefore, a small amount of the EG was additionally charged to form dense char layer using its 2D shape. When the EG and MOSw are used together, the cooling and diluting effects from MOSw and a blocking effect by a dense char layer formation from the EG were generated appropriately. As a result, high flame retardancy of V-0 grade can be achieved by a synergistic effect between the MOSw and EG, while maintaining excellent mechanical strength.

ACKNOWLEDGEMENT

This study was conducted with the support of the Dansuk.

REFERENCES

1. Ning, Q.G., and Chou, T.W., "A Closed-Form Solution of the Transverse Effective Thermal Conductivity of Woven Fabric Composites," *Journal of Composite Materials*, Vol. 29, No. 17, 1995, pp. 2280-2294.
2. Park, Y.B., Yang, H.J., Kweon, J.H., Choi, J.H., and Cho, H.I., "Failure of Composite Sandwich Joints under Pull-out Loading," *Composites Research*, Vol. 24, No. 1, 2011, pp. 17-23.
3. Vinson, J.R., "The Behavior of Sandwich Structures of Isotropic and Composite Materials," Routledge, 2018.
4. Jeong, K.W., Park, Y.B., Choi, J.H., and Kweon, J.H., "A Study on the Failure Mode and Load of the Composite Key Joint," *Journal of Composite Materials*, Vol. 48, No. 12, 2014, pp. 1417-1427.
5. Prabhakar, M.N., Shah, A.U.R., and Song, J.I., "A Review on the Flammability and Flame Retardant Properties of Natural Fibers and Polymer Matrix Based Composites," *Composites Research*, Vol. 28, No. 2, 2015, pp. 29-39.
6. Cartié, D.D., "Effect of z-fibresTM on the Delamination Behaviour of Carbon-fibre/epoxy Laminates," Doctoral Dissertation, Cranfield University, 2000.
7. Seidi, F., Movahedifar, E., Naderi, G., Akbari, V., Ducos, F., Shamsi, R., Vahabi, H., and Saeb, M.R., "Flame Retardant Polypropylenes: A Review," *Polymers*, Vol. 12, No. 8, 2020, p. 1701.
8. He, W., Song, P., Yu, B., Fang, Z., and Wang, H., "Flame Retardant Polymeric Nanocomposites through the Combination of Nanomaterials and Conventional Flame Retardants," *Progress in Materials Science*, Vol. 114, 2020, 100687.
9. Lee, D.W., Park, S.B., and Song, J.I., "Study on Mechanical Properties and Flame Retardancy of Polypropylene Based Self-reinforced Composites," *Composites Research*, Vol. 30, No. 3, 2017, pp. 223-228.
10. Kim, J., and Ku, B.C., "A Review of Flame Retarding Polyacrylonitrile (PAN) Fibers and Composites," *Composites Research*, Vol. 32, No. 6, 2019, pp. 342-348.
11. Mun, S.Y., Lee, S.Y., and Lim, H.M., "Flame Retardant Properties of Basalt Fiber Reinforced Epoxy Composite with Inorganic Fillers," *Composites Research*, Vol. 32, No. 6, 2019, pp. 368-374.